

# Viscous potential flow analysis of peripheral heavy ion collisions

D.J. Wang<sup>1</sup>, Z. Nédá<sup>2</sup>, and L.P. Csernai<sup>1</sup>

<sup>1</sup> *Department of Physics and Technology, University of Bergen, Allegaten 55, 5007 Bergen, Norway*

<sup>2</sup> *Department of Physics, Babeş-Bolyai University, Cluj, Romania*

(Dated: May 23, 2022)

The conditions for the development of a Kelvin-Helmholtz Instability (KHI) for the Quark-gluon Plasma (QGP) flow in a peripheral heavy-ion collision is investigated. The projectile and target side particles are separated by an energetically motivated hypothetical surface, characterized with a phenomenological surface tension. In such a view, a classical potential flow approximation is considered and the onset of the KHI is studied. The growth rate of the instability is computed as function of phenomenological parameters characteristic for the QGP fluid: viscosity, surface tension and flow layer thickness.

PACS numbers: 47.20.Ft, 24.85.+p, 25.75.Ld, 12.38.Mh

## I. INTRODUCTION

The first models of high energy heavy ion collisions in the 1970s were successful by assuming highly idealized shock fronts where the matter was heated up and compressed in a front (having a discontinuity in perfect fluid flow [1, 2]). This led to high pressured, shock compressed domains which collectively deflected the incoming nuclear fluid. The observation of this directed flow (side splash of bounce-off) was the first proof of the collective fluid dynamical behaviour of nuclear matter [3]. Recent theoretical developments and experimental observation of high multiplicity fluctuations indicate that the QGP is a low viscosity fluid, which makes turbulent phenomena possible [4–6]

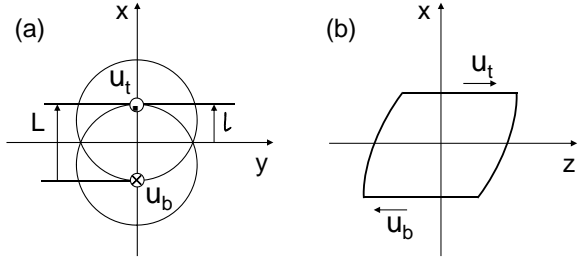


FIG. 1. Sketch of a collision: (a) is a view in the transverse,  $[x,y]$  plane and (b) is an illustration in the reaction,  $[x,z]$  plane. The almond shape in the middle of figure (a) is the participant zone of the event. Right after the collision, streaks are formed and the top streaks move along the  $z$  direction while bottom ones move along the  $-z$  direction. Due to this velocity shear, an instability wave will appear on the interface plane between the top and bottom sheets.

Here we adopt again a fluid dynamical picture and discuss the strong shear flow arising in the initial states of peripheral heavy ion collisions at ultra-relativistic energies, which may lead to KHI under favorable conditions, as discussed recently [4].

A simple analytic study showing the development of the KHI in a highly idealized situation is discussed. The

investigated phenomenon has some resemblance to the initial state of a peripheral heavy ion collision. In these collisions the collective flow should be a "shear flow" because the top participant layers, move nearly with projectile velocity while the bottom layers with the target velocity.

In the reaction plane, the height of the participant profile is  $L = 2R - b$ , where  $b$  is the impact parameter, and the half height is  $l = L/2 = (2R - b)/2$ . In the following we will denote by  $n$  the nuclear matter density and by  $\eta$  its phenomenological viscosity. The matter coming from different sources is marked by subscript/superscript  $t$  (top) and  $b$  (bottom), see Fig. 1.

For simplicity reasons we consider a two dimensional non-relativistic dynamics in the reaction plane. The position vector is  $\mathbf{x} = (x, z)$ , and the velocity vector is  $\mathbf{v} = (v_x, v_z)$ .

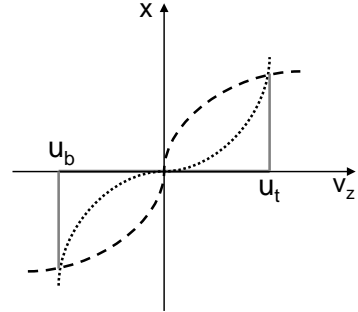


FIG. 2. The velocity along the  $z$  axis, is represented by the dotted curve, calculated in our CFD model and presented in Ref. [4]. The full line with two singularities in its derivative is the case used in Ref. [7]. Here we have to mention that the velocity profile of the dotted curve will induce the KHI effect, while the velocity profile illustrated with the dashed curve will not, see chapter 8 of Ref. [8].

The nearly perfect QGP provides a possibility of a strong idealization in this situation. The velocity profiles for  $v_z$  presented on Fig. 2 illustrates (the dotted line) that the KHI develops if we have a strong shear flow at the  $x = 0$  plane, which leads to large vorticity and circulation. With decreasing viscosity we could idealize this

configuration in a way that the vorticity is constrained into a narrow layer around the  $x = 0$  plane, while the circulation remains constant. In a limiting case if we constrain the vorticity and shear to the dividing,  $x = 0$ , plane, this plane would represent an infinite vorticity, providing the same circulation for a trajectory surrounding the dividing plane.<sup>1</sup> In this limiting case the velocity profile is idealized to the one indicated by the full line in Fig. 2. Thus in the top and bottom domain the flow has no shear, and can be described as potential flow, which is an important simplification and idealization. This makes the analytic study of the KHI possible.

## II. THE ANALYTIC MODEL

Thus, the idealized dividing layer represents a discontinuity of the flow velocity (i.e. unconstrained slip). At the same time a small viscosity would contribute the transverse momentum transfer to a small distance across the dividing front. The particles in this narrow layer, scattering over from the other side of the dividing plane, would have a high relative velocity, so this layer would exhibit an extra energy increase compared to the general fluid body on the top or the bottom side of our system. This can be taken into account as an effective surface energy of the dividing layer. This surface energy can be estimated both from a microscopic kinetic theory approach, or from a rough energy balance calculation. In a microscopic approach one would assume that the this extra energy depends on the (viscosity dependent) thickness of the layer and the (temperature dependent) rate of transverse flow crossing the dividing plane. A quantitative estimate of this surface energy in this idealized situation is not feasible, but its existence and a rather qualitative estimate can be made. In contrast with this, a phenomenological energy balance calculation is easier to perform. The advantage of such an approach would be that one does not rely on further estimates for the involved physical parameters. Here, we will use this later method to approximate the surface tension of the dividing layer.

Following ref. [7] we idealize the problem and assume an initial state where the shear is localized at the dividing plane between the top (t) half and the bottom (b) half of the fluids, in order that we can use the potential flow description in the top and bottom parts of the fluid, see Fig. 3. We assume that the fluid in the top and bottom parts are allowed to slip at the top and bottom boundaries as well as at the dividing surface between them. We will reference these as unconstrained slip-conditions. The initial flow velocity is assumed to be uniform in the two layers, so that for the top layer  $\mathbf{v}^t = (0, U_t)$  for  $0 < x < l$  and

for the bottom layer  $\mathbf{v}^b = (0, U_b)$  for  $-l < x < 0$  initially. This means that initially the amplitude of the wave-like instability is extremely small, and we are looking for the conditions to have a growing amplitude for this instability. For the sake of analytic model we assume that the density is constant. Numerical studies [4] show that this constraint can be relaxed.

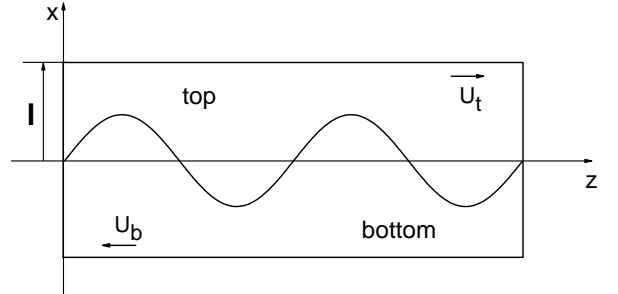


FIG. 3. The profile of the top and bottom fluids layers with a dividing surface wave on it. The top external fluid moves with velocity  $U_t$  along the  $z$ -direction, while the bottom fluid moves with velocity  $U_b$  along  $-z$ -direction. The slip is unconstrained at the dividing surface.

Just as in ref. [4] we will use an average energy and mass density for our estimates. Since the effective particle density is constant the continuity equation of the flow velocity,  $\mathbf{v}$ , will become:

$$\nabla \cdot \mathbf{v} = 0. \quad (1)$$

For the top and bottom parts of the fluid we assume small velocities and neglect velocity gradients and we assume that the rotation of the flow velocity is  $\nabla \times \mathbf{v} = 0$ . Under such conditions we can describe the flow as a potential flow, i.e.,  $\mathbf{v} = \nabla \phi$ , where  $\phi$  is the velocity potential,  $\phi \equiv \phi(t, x, z)$ . The continuity equation is  $\Delta \phi \equiv \nabla^2 \phi = 0$ , applied this for the top and bottom layers gives:

$$\nabla^2 \phi_t = 0 \text{ for } 0 < x < l, \quad (2)$$

$$\nabla^2 \phi_b = 0 \text{ for } -l < x < 0. \quad (3)$$

We assume that due to the raising instability the initially plane interface will experience a perturbation and will deviate from the  $x = 0$  plane. The height of the deviation from the  $x = 0$  plane is denoted by  $h = h(t, z)$ , and it is taken as wave-like perturbation in the  $z$  direction with wave-number  $k$ . We also allow the amplitude at a given coordinate to change in time. The most general form for such a wave-like interface would be

$$h(t, z) = A_0 e^{(\sigma t + ikz)}, \quad (4)$$

where,  $\sigma$  is the complex growth-rate, and  $A_0$  is a complex amplitude.

Consequently, the fluid on the top and bottom sides next to the dividing surface will have vertical velocity

<sup>1</sup> The conservation of circulation occurs in classical, barotropic flow. In QGP the temperature dominates the pressure change, so the circulation is not conserved but decreases during the expansion of the system [9].

components:

$$v_x^{t,b} = \frac{dh}{dt} = \frac{\partial h}{\partial t} + U_{t,b} \frac{\partial h}{\partial z}, \quad (5)$$

where  $U_t$  and  $U_b$  are the flow velocities of the fluid at the top and bottom of the bounding surfaces, respectively. These are assumed to be the average velocity of the fluids at the surface neglecting the horizontal velocity fluctuations arising from wave formation. Initially these velocity fluctuations are small, and our aim is to study the initial development of KHI. At the  $h(t, z)$  dividing surface we also assume unconstrained slip conditions of the two inversely flowing fluid slabs.

The boundary conditions for the external border of the profile are:

$$v_x^{t,b} = \frac{\partial \phi_{t,b}}{\partial x} = 0 \text{ at } x = \pm l, \quad (6)$$

Initially (at time  $t = 0$ ), one would also have to satisfy:

$$v_z^{t,b}(t = 0, x = \pm l) = U_{t,b} \quad (7)$$

At each time moment the potential  $\phi_t$  and  $\phi_b$  is satisfying Eq. (2,3,5,6) for the top and bottom sides respectively:

$$\begin{aligned} \frac{\partial^2 \phi_{t,b}}{\partial x^2} + \frac{\partial^2 \phi_{t,b}}{\partial z^2} &= 0 \\ v_x^{t,b} = \frac{dh}{dt} = \frac{\partial h}{\partial t} + U_{t,b} \frac{\partial h}{\partial z} &\text{ at } x = 0, \\ v_x^{t,b} = \frac{\partial \phi_{t,b}}{\partial x} &= 0 \text{ at } x = \pm l. \end{aligned} \quad (8)$$

Assuming for the interface,  $h(t, z)$ , in Eq. (4), a wave-like perturbation, which is symmetric in  $\pm x$  and exponentially decreasing away from the surface, the solution can be searched in the form:

$$\phi_{t,b} = A_{t,b} \cosh[k(x-l)]e^{(\sigma t + ikz)} + zU_{t,b}, \quad (9)$$

where  $A_t$ ,  $A_b$  and  $A_0$  are the complex amplitudes,  $\sigma$  is the growth rate and  $k$  is the wave number. From the kinematic conditions on the dividing layer Eq. (5), we get the following equations at the dividing surface:

$$(\sigma + ikU_{t,b})A_0 = \mp kA_{t,b} \sinh(kl) \quad (10)$$

The pressure ( $p$ ), viscosity ( $\eta$ ) and surface tension ( $\gamma$ ) balance at the interface writes as:

$$-p_t + 2\eta \frac{\partial v_x^t}{\partial x} - (-p_b + 2\eta \frac{\partial v_x^b}{\partial x}) = -\gamma \frac{\partial^2 h}{\partial z^2}, \quad (11)$$

The surface energy and consequently the surface tension of the dividing layer will be approximated later. As it was already emphasized in the introductory paragraphs, although the top (t) and bottom (b) sides are of the same nuclear matter, the velocity jump or the sharp velocity change contribute to additional surface energy due to the large shear at the interface exhibiting extra energy or to a smaller extent by the momentum dependance of nuclear interaction potential.

Since we have unconstrained slip conditions on the dividing surface between the top and bottom layer,  $p_t$  and  $p_b$  can be written by the classical equation of motion without the viscous term as:

$$\rho \left( \frac{\partial v_z^{t,b}}{\partial t} + U_{t,b} \frac{\partial v_z^{t,b}}{\partial z} \right) = -\frac{\partial p_{t,b}}{\partial z}, \quad (12)$$

Then, first we apply  $\nabla_z$  on both sides of the equation and substitute equation of continuity,  $\partial_z v_z = -\partial_x v_x$ , into it:

$$\rho \left( \frac{\partial^2 v_x^{t,b}}{\partial t \partial x} + U_{t,b} \frac{\partial^2 v_x^{t,b}}{\partial x \partial z} \right) = \frac{\partial^2 p_{t,b}}{\partial z^2}. \quad (13)$$

Here  $\rho$  is the effective mass density of the QGP, we use  $\rho = 10 \text{ GeV}/\text{fm}^3 c^2$  [4] in our work. In order to substitute the above equations into Eq. (11), we consider the second order derivative of Eq. (11) as a function of  $z$ , and substitute Eq. (13) into it. Thus the pressure, viscosity and surface tension balance will be written in the following form:

$$\begin{aligned} &-\rho \left( \frac{\partial^2 v_x^t}{\partial t \partial x} + U_t \frac{\partial^2 v_x^t}{\partial x \partial z} \right) + 2\eta \frac{\partial^3 v_x^t}{\partial x \partial z^2} + \\ &\rho \left( \frac{\partial^2 v_x^b}{\partial t \partial x} + U_b \frac{\partial^2 v_x^b}{\partial x \partial z} \right) - 2\eta \frac{\partial^3 v_x^b}{\partial x \partial z^2} = -\gamma \frac{\partial^4 h}{\partial z^4}. \end{aligned} \quad (14)$$

By inserting the velocity derived from Eq. (9) and the considered interface profile, Eq. (4), into the above equation, and expressing the top and bottom amplitudes,  $A_{t,b}$  from Eq. (10), after simplifying all over with  $A_0$ , and putting the condition  $x = 0$ , we obtain an equation for  $\sigma$  and  $k$ :

$$\begin{aligned} &[\rho(\sigma + ikU_t)^2 + 2\eta k^2(\sigma + ikU_t)] \coth(kl) \\ &+ [\rho(\sigma + ikU_b)^2 + 2\eta k^2(\sigma + ikU_b)] \coth(kl) \\ &+ \gamma k^3 = 0. \end{aligned} \quad (15)$$

Considering this as an equation for  $\sigma$ , one can write it in a simplified form as

$$A\sigma^2 + 2B\sigma + C = 0, \quad (16)$$

where the coefficients,  $A, B, C$  are defined as:

$$\begin{aligned} A &= 2\rho \coth(kl), \\ B &= 2k^2\eta \coth(kl) + ik\rho(U_b + U_t) \coth(kl) \\ &= B_R + iB_I, \\ C &= -k^2\rho \coth(kl)(U_t^2 + U_b^2) + \gamma k^3 \\ &+ 2ik^3\eta \coth(kl)(U_t + U_b) = C_R + iC_I. \end{aligned} \quad (17)$$

The solution is

$$\begin{aligned} \sigma &= -\frac{B}{A} \pm \sqrt{\frac{B^2}{A^2} - \frac{C}{A}} \\ \rightarrow \sigma_R + i\sigma_I &= -\frac{B_R + iB_I}{A} \pm \frac{\sqrt{D}}{A}, \end{aligned} \quad (18)$$

where  $D = D_R + iD_I$  and

$$\begin{aligned} D_R &= k^2\rho^2 \coth^2(kl)(U_t - U_b)^2 \\ &+ 4\eta^2 k^4 \coth^2(kl) - 2\rho \coth(kl)\gamma k^3, \\ D_I &= 0, \end{aligned} \quad (19)$$

thus the real part and the imaginary part can be expressed as:

$$\sigma_R = \frac{-B_R \pm \sqrt{D_R}}{A}, \quad \sigma_I = -\frac{B_I}{A}. \quad (20)$$

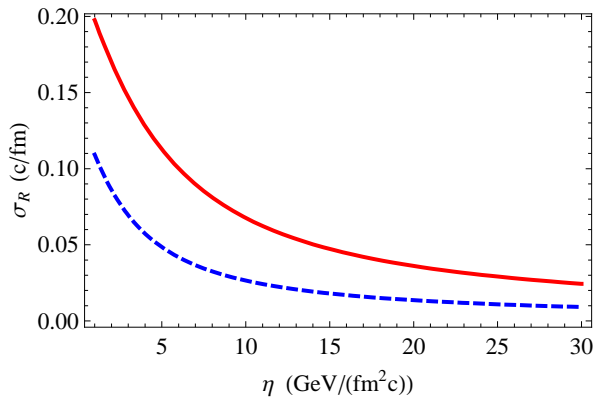


FIG. 4. (color online) The real part of the growth rate,  $\sigma_R$ , is shown as function of the viscosity  $\eta$ . The full (red) line is for the surface tension  $\gamma = 0.4 \text{ GeV/fm}^2$  and the dashed (blue) line is for  $\gamma = 3.5 \text{ GeV/fm}^2$ . The wave number,  $k$ , is taken to be  $k = 0.6 \text{ fm}^{-1}$  and the effective mass density is  $\rho = 10 \text{ GeV/fm}^2 \text{ c}^2$ . The growth rate decreases when the viscosity increases suggesting that the KHI grows weaker for a more viscous fluid.

In heavy ion collisions, the matter will expand after the collision, and in fact there is no external boundary (top and bottom) of the fluid shown in Fig. 3. If we assume  $l \rightarrow \infty$ , the above equations can be simplified as:

$$\sigma_R = -\frac{k^2 \eta}{\rho} \pm \sqrt{\frac{k^4 \eta^2}{\rho^2} + \frac{k^2 (U_t - U_b)^2}{4} - \frac{\gamma k^3}{2\rho}}, \quad (21)$$

$$\sigma_I = -\frac{k(U_t + U_b)}{2}. \quad (22)$$

In Eq. (21), for the typical parameters of a peripheral heavy ion collision, the real part of the growth rate,  $\sigma_R$ , is dominantly dependent on the viscosity  $\eta$ , namely the first term and the first term in the square root. In our expanding system the dominant wave number of KHI is changing with time.

### III. RESULTS

According to the CFD observations [4], initially we have a small wave formation with  $k \approx 1 \text{ fm}^{-1}$ , but with time and expansion, the possible largest wave length takes over with  $k \approx 0.6 \text{ fm}^{-1}$ , which decreases further with the expansion of the system. By assuming  $|U_t - U_b| = 0.8 \text{ c}$ , we can obtain the growth rate dependence of the viscosity,  $\eta$ , and the surface tension,  $\gamma$ , which are shown in Figs. 4 and 5.

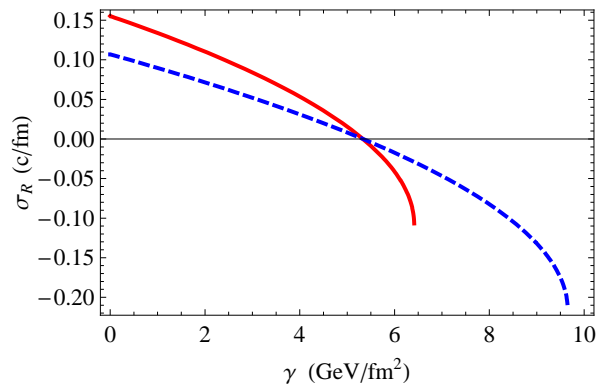


FIG. 5. (color online) The real part of the growth rate,  $\sigma_R$ , as a function of the surface tension  $\gamma$  with different values of viscosity  $\eta$ . The full (red) line represents  $\eta = 3 \text{ GeV/fm}^2$  and the dashed (blue) line represents  $\eta = 6 \text{ GeV/fm}^2$ . The wave number  $k$  is taken as  $0.6 \text{ fm}^{-1}$  and the effective mass density  $\rho$  is  $10 \text{ GeV/fm}^2 \text{ c}^2$ . As we can see in the figure, the two curves cross each other at  $\sigma_R = 0$ , which is around  $\gamma = 5.3 \text{ GeV/fm}^2$ , and then the growth rate becomes negative. With bigger surface tension the KHI effect is less probable to appear.

Similarly to the viscosity the effective surface energy also influences the growth rate of KHI. As expected larger surface tension or surface energy damps the growth of KHI. Beyond a critical surface energy (in our model at  $\gamma_{crit} \approx 5.3 \text{ GeV/fm}^2$ ) the surface tension will lead to a decrease in the KHI. Interestingly this threshold value is independent of the viscosity. This is part of the general feature that the behavior of the zero-growth ( $\sigma_R = 0$ ) curve is independent of the value of the viscosity in this model. The growth rate and damping rate are of course depend on the viscosity.

The condition to have a growing instability is to have a solution with  $\sigma_R > 0$ . Taking into account that  $D$  is a real number ( $D_I = 0$ ,  $D_R > 0$ ), and  $B_R > 0$ , from (20) it follows that in order to have a positive growth rate, ( $\sigma_R > 0$ ), one has to satisfy the condition:

$$\sqrt{D_R} > B_R. \quad (23)$$

Thus, using (17) and (19) we get the condition for positive growth:

$$V^2 > \frac{2\gamma k}{\rho \coth(kl)}, \quad (24)$$

where  $V \equiv U_t - U_b$ .

The above condition will limit the region of the  $(V, k)$  parameter space where the KHI can evolve. One should also keep in mind the results obtained in [4], regarding the acceptable wave numbers,  $k$ , for the considered wave-like instability. Definitely there is a lower cutoff ( $k_{min}$ ) governed by the beam-directed longitudinal length of the

flow,  $l_z$ :

$$k_{min} = \frac{2\pi}{l_z} \quad (25)$$

For the  $b = 0.5b_{max}$  and  $b = 0.7b_{max}$  impact parameter values the calculations in [4] leads to  $k_{min} = 0.598 \text{ fm}^{-1}$  and  $k_{min} = 0.479 \text{ fm}^{-1}$  values, respectively. There is also an upper limit for the wave-numbers,  $k_{max}$  governed by the Kolmogorov length scale,  $\lambda_K$ :

$$k_{max} = \frac{2\pi}{\lambda_K} \quad (26)$$

According to [4] this characteristic length-scale is estimated for the above given impact parameters as:  $\lambda_K \approx 3.5 \text{ fm}$  and  $\lambda_K \approx 2.5 \text{ fm}$ , leading to  $k_{max} = 1.79 \text{ fm}^{-1}$  and  $k_{max} = 2.51 \text{ fm}^{-1}$  values, respectively.

For the peripheral Pb+Pb collisions, the radius of Pb is  $R = 7 \text{ fm}$ , thus  $b_{max} = 14 \text{ fm}$ . In order to get the parameter space where the KHI will growth let us estimate now the value of the surface tension. As it has been discussed in the introductory part this surface energy comes from the energy excess of the unbalanced energy flow in the two layers. Although a theory based on kinetic considerations would capture more from the involved physics, here we just consider a simple approach based on the energy balance. The reason for doing this is that less number of phenomenological parameters are needed.

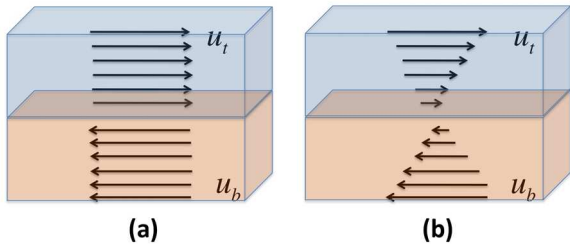


FIG. 6. Two different velocity profiles: (a) is the profile used in our present work, it has two distinct layers with two constant velocity  $U_t$  and  $U_b$ , while (b) has a flow transition from the two layers, and at the diving surface the velocity is smallest.

The flow assumed in the present work has a perpendicular velocity profile illustrated in Fig. 6a. This means that a smooth velocity profile (Fig. 6b), characterizing a stable and balanced viscous flow is not formed. In the case illustrated in Fig. 6a one would assume that there are two distinct layers flowing with velocities  $U_t$  and  $U_b$ . For the balanced flow illustrated in Fig. 6b, one would observe a smooth flow velocity transition from  $U_t$  to  $U_b$ . It is obvious that in the laboratory frame, this later flow has less kinetic energy in the  $z$  direction than the previous one. The difference between the two kinetic energies can be accounted as the energy surplus of the dividing layer. If we denote the contact surface between the flows in the top and bottom layers by  $S$ , the surface tension could be estimated as

$$\gamma = \frac{E_{kz}^a - E_{kz}^b}{S}, \quad (27)$$

where  $E_{kz}^{a,b}$  denotes the kinetic energy of the flow in the  $z$  direction for the profile illustrated in Fig. 6a and 6b, respectively. The total relativistic kinetic energy of the system,  $E_k$  in the laboratory frame is

$$E_k = 2M_{Pb}c^2 \left( \frac{1}{\sqrt{1 - \frac{V^2}{c^2}}} - 1 \right), \quad (28)$$

where  $V = U_t - U_b$  is the relative speed of the two projectiles, and  $M_{Pb}$  is the mass of the collided Pb ions. Assuming that the participating zone in the collision has a surface  $q \times \pi R^2$ , (the overlapping regions are only a  $q$  part of the possible ones) and the kinetic energy of the participating particles in this zone is distributed equally in all the directions of the space, a rough approximations for  $E_{kz}^a$  would be:  $E_{kz}^a = q \frac{E_k}{3}$ . On the other hand, for the flow illustrated in Fig. 6b, due to the balanced velocity profile, a part of this kinetic energy has to be dissipated, and assuming a linear velocity profile one gets:  $E_{kz}^b = 1/2 E_{kz}^a$ . The above arguments lead us to a first approximation of the surface tension value:

$$\gamma = \frac{q}{3} \frac{M_{Pb}c^2}{S} \left( \frac{1}{\sqrt{1 - \frac{V^2}{c^2}}} - 1 \right). \quad (29)$$

Assuming  $q \approx 0.5$  and estimating the surface of the dividing layer,  $S$ , from [4], one gets the values of  $\gamma$  for different impact parameter values.

The surface tension is estimated to be  $\gamma = 0.4 \text{ GeV/fm}^2$  from Eq. (29). This value is used in the following examples. The critical velocity Eq. (24) for different impact parameters is shown in Fig. 7. These curves show the border of instability of the growth rate,  $\sigma_R$ . The curves divide the space into two areas, the upper side above the curve is the region where the instability grows and the area below the critical velocity curve is where the instability does not grow. The KHI development region is also limited by the  $k_{min}$  and  $k_{max}$  values as drawn in figure Fig. 7.

The above consideration is for  $\sigma_R = 0$ , however, this does not show the  $\eta$ -dependence of the growth. In order to see how the instability depends on the viscosity,  $\eta$ , we can cast Eq. (20) into the form:

$$\sigma_R = \frac{k^2 \eta}{\rho} \left[ -1 \pm \sqrt{1 + \frac{\rho}{\eta^2} \left( V^2 \rho - \frac{\gamma k}{\coth(kl)} \right)} \right]. \quad (30)$$

This suggests that with our characteristic parameters the dependence on the thickness of the fluid layer,  $l$ , is weak as shown in Fig. 8.

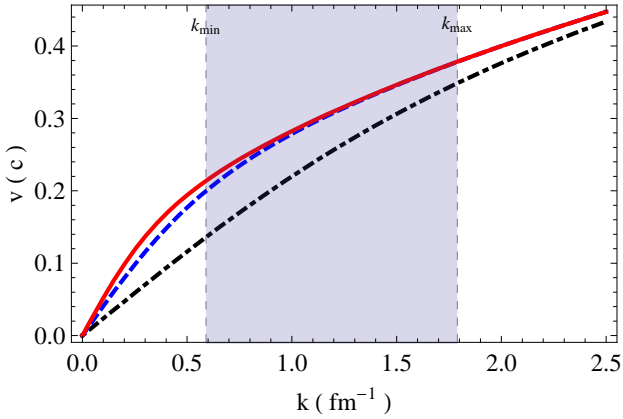


FIG. 7. (color online) The critical velocity  $V \equiv U_t - U_b$  as function of the wave number, at the condition of vanishing growth rate,  $\sigma_R = 0$ . The red full line, blue dashed line and black dot-dashed line are for impact parameters  $b = 0.5, 0.7, 0.9 b_{max}$ , respectively. On the graph we also illustrated the two natural boundaries  $k_{min}$  and  $k_{max}$  for  $b = 0.5 b_{max}$ . The KHI will evolve thus above the critical velocity curves and between these two limits. For increasing impact parameters, the instability is less able to grow and the system tends to be stable.

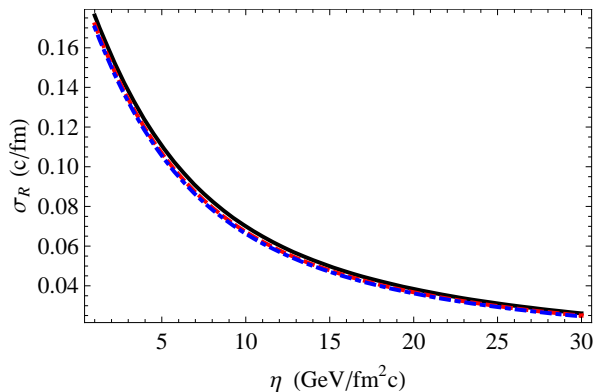


FIG. 8. (color online) The growth rate  $\sigma_R$  as a function of the viscosity  $\eta$  at different values of  $l$ , black line is for  $l = 0.1$  fm, the red dashed line is for  $l = 2$  fm and the blue dot-dashed line is for  $l = \infty$ . The wave number is  $k = 0.6$  fm $^{-1}$ , the surface tension is  $\gamma = 0.4$  GeV/fm $^2$ , the relative velocity is  $V = 0.8$  c and  $\rho = 10$  GeV/fm $^2$  c $^2$ . The growth rate depends weakly on  $l$ , while it depends significantly on the viscosity, increasing strongly for small viscosity values.

#### IV. CONCLUSIONS

In classical gravitational water waves the wave formation and wave speed depends strongly on the depth of the

water, i.e. the layer thickness,  $l$ . In a heavy ion collisions the role of the layer thickness is different. The material properties of the top and bottom layers are not different, these are separated from another by the relatively thin layer of large shear. Still the occurrence of KHI in such conditions is not uncommon as it is frequently observed, as turbulence during airplane flights, or it is even visible if the air has high humidity and the condensation makes the KHI visible.

In peripheral heavy ion collisions the layer thickness is given in the initial state, but there is no solid boundary and the system expands in all directions. Thus, for this physical situation the large or infinite layer thickness is more relevant in this model, even if the initial layer thickness is finite and usually smaller than the longitudinal size of the initial state.

Large viscosity or the corresponding low Reynolds number prevent the development of turbulence and KHI, so that these phenomena appear only above a critical Reynolds number. This critical Reynolds number depends on the flow configuration, so it is separately analysed for the KHI also, see ref. [4]. The present study confirms that the dependence of the growth rate on the viscosity reflects the usual tendency that instability and turbulence increases with smaller viscosity.

When the KHI develops between two fluids (e.g. air/water or air/oil) the large surface tension difference at the interface damps the development of the instability, this is well known for sailors for centuries. If KHI develops inside one fluid, like in air or in quark gluon fluid, there is no surface tension in the classical sense, but the layer with large shear has extra energy, and it leads to an effective surface tension, which hinders the development of KHI.

We presented a strongly idealized analytic model for the development of the Kelvin-Helmholtz Instability in ultra-relativistic heavy ion reactions. We compressed the shear zone into a central infinitesimal layer, following the idea of ref. [7], and assumed that the remaining flow can be approximated as potential flow. The idealized dividing layer was attributed a surface energy and unconstrained slip between the top and bottom fluid layers. It is interesting that in this model the KHI is developing under similar conditions, as in numerical high resolution relativistic fluid dynamical calculations [4]. This model also shows that critical size KHI may occur for low viscosity QGP.

*Acknowledgement* The work of Z.N. was supported by the exploratory "Ideas" research grant: PCE-IDEI-0348/2011.

[1] W. Scheid, H. Müller and W. Greiner, Phys. Rev. Lett. **32** (1974) 741, and W. Scheid and W. Greiner, Z. Phys.

**226** 365 (1969).

[2] G.F. Chapline, M.H. Johnson, E. Teller and M.S. Weiss,

- Phys. Rev. **D8** (1973) 4302.
- [3] H.Å. Gustafsson, H.H. Gutbrod, B. Kolb, H. Lohner, B. Ludewigt, A.M. Poskanzer, T. Renner, H. Riedesel, H.G. Ritter, A. Warwick, F. Weik and H. Wieman, Phys. Rev. Lett. **52** (1984) 1590.
- [4] L.P. Csernai, D.D. Strottman and C. Anderlik, Phys. Rev. C **85**, 054901 (2012).
- [5] A. Bonasera, Nuovo Cimento, 109 A, 1405 (1996).
- [6] Stefan Floerchinger and Urs Achim Wiedemann, Journal of High Energy Physics, doi:10.1007/JHEP 11, 100 (2011); and J. Phys. G: Nucl. Part. Phys. 38, 124171 (2011).
- [7] T. Funada and D. D. Joseph, J. Fluid. Mech. **445**, 263-283 (2001).
- [8] P.G.Darzin, Introduction to Hydrodynamic Stability, Cambridge University Press, P145 (2002).
- [9] L.P. Csernai, V.K. Magas, and D.J. Wang, Submitted to Phys. Rev. C [CY10249] (2013).